CO(v,J) Product State Distributions from the Reaction $O(^3P) + OCS \rightarrow CO + SO$

Scott L. Nickolaisen[a], Harry E. Cartland[b], David Veney[b], and Curt Wittig

Department of Chemistry
University of Southern California
Los Angeles, CA 90089-0482
(213)740-7760

(a) current address: Jet Propulsion Laboratory, MS 183-901, 4800 Oak Grove Drive, Pasadena, CA 91109

(b) Science Research Laboratory, U.S. Military Academy, West Point, NY 10996

ABSTRACT

The title reaction was studied by probing the CO(v,J) product state distributions. Oxygen atoms were formed by 355 nm photolysis of NO_2. Photolysis produces approximately equal populations of NO(v=0) and NO(v=1). The collision energy of oxygen atoms corresponding to NO(v=0) is 1570 cm^{-1}. This is above the O + OCS activation barrier of 1540 cm^{-1}. Oxygen atoms corresponding to NO(v=1) do not have sufficient energy to proceed over the activation barrier, thus insuring monoenergetic collisions. CO product was probed using an IR tunable diode laser. Nascent CO distributions were extracted from the transient absorption signals using an initial slope approximation. A vibrational branching ratio of $[v=1]/[v=0] \leq 0.05$ was measured. $CO(v \geq 2)$ was not detected. The CO(v=0) rotational Boltzmann plot was bimodal. The distribution for $0 \leq J \leq 15$ had a temperature of 350 ± 20 K. For $J \geq 15$, the plot had a temperature of 4400 ± 390 K. The low J population is the result of rotational relaxation of the nascent CO distribution. The high J signals are direct measure of the nascent CO population. Surprisal analysis resulted in a parameter of $\Theta_R = 3.7 \pm 0.5$. Hence, the CO(v=0) distribution is colder than a "prior" statistical model.

1. INTRODUCTION

The reaction of atomic oxygen and carbonyl sulfide has been examined to a degree in the past. Interest in the title reaction stems from its involvement in both atmospheric and combustion chemistry of sulfur containing systems.[1] The kinetics of the reaction have been previously studied yielding an expression for the rate constant of $k = 2.35 \times 10^{-11} \exp\{-1540\ cm^{-1}/kT\}\ cm^3\ molecule^{-1}\ s^{-1}$.[2] However, the details of the potential energy surface (PES) for this system have not been determined. For example, it is unknown whether the activation barrier of 1540 cm^{-1} represents a saddle point on the potential energy

 0-8194-0784-4/92/$4.00

surface, or if a minimum exists along the reactive pathway which corresponds to an activated intermediate.

Our examination of the O + OCS reaction is an extension of a set of experiments in which several analogous atom-molecule reactions have been studied. Other systems studied were the H + CO_2 and H + OCS reactions.[3,4] The ultimate goal of these studies is to understand the factors which determine the partitioning of energy in the reaction products. These factors include the energy of the reactive collision, the shape of the PES along the reactive pathway, and the endothermicity or exothermicity of the reaction. The product state distributions determined in these reactions can yield information about the location of the transition state, the extent of energy randomization within the products, and the possible role of reactive intermediates.

2. EXPERIMENTAL

The basic experimental approach of these studies has been outlined previously.[3,4] Atomic oxygen was generated by photolysis of NO_2 using the 355 nm output of a tripled Nd:YAG laser (Quantel, model YG581C). UV pulse energies were measured by a photodiode and were typically 150 mJ. NO_2 (Matheson) was purified by successive freeze/pump/thaw cycles in an ethanol/liquid nitrogen. OCS (Matheson) was purified from CO contamination by condensing OCS in an ethanol/liquid nitrogen slush (157 K) and pumping off the head gas. A mixture of 20% NO_2 in OCS was prepared and allowed to thoroughly mix. The gas mixture was flowed through a 2 m Pyrex cell at a total pressure of 400 mTorr.

CO(v,J) product was monitored by a tunable IR diode laser (Laser Analytics system). Because the diode laser has no internal wavelength calibration, it was necessary to use a reference cell in order to provide an absolute wavelength marker. To accomplish this, 10% of the IR beam was directed to a reference cell which consisted of a water cooled Pyrex tube mounted with CaF_2 windows and equipped with high voltage electrodes. A mixture of CO in helium was flowed through the electrical discharge cell. By adjusting the current and voltage of the discharge, CO rotational lines in vibrational levels up to $v \approx 9$ could be found. The diode laser wavelength was locked to the desired CO reference line by dithering the frequency over a very small range. The output of the reference cell detector was connected to a lock-in amplifier which was configured to take the first derivative of the incoming signal. The lock-in amplifier output was attenuated and connected to the external input of the diode laser current. The lock-in output acted as a correction signal to compensate for drift of the diode laser frequency away from line center.

The remainder of the IR beam was passed through the reaction cell collinear with the UV photolysis beam. The UV beam was separated from the IR beam by a dichroic mirror. The IR beam was passed through a 3.5 - 6.5 μm bandpass filter and focused onto a .25 mm diameter photovoltaic InSb detector (Judson, model J10D-M204) with an impedance matched preamplifier (Perry, model 730-40). The detection system had a measured response time of ~ 70 ns. The signal from the reaction cell detector was digitized by a 100 Megasample s^{-1} transient recorder (LeCroy, model 8818A). Triggering of the

transient recorder was synchronized to the photolysis pulse using the trigger signal of the Nd:YAG laser. Experiments were performed at repetition rate of 0.5 Hz, and 200 transients were averaged for each recorded signal.

3. RESULTS AND DISCUSSION

The reaction of ground state atomic oxygen and carbonyl sulfide has an exothermicity of $\Delta H_{f,298} = -211.4$ kJ mol^{-1}. The system has an activation barrier of 1540 cm^{-1} to reaction. In a study of the photolysis of NO_2 at 347 nm, it was found that NO(v=0) and NO(v=1) were produced in approximately equal amounts.[5] This is expected to hold for 355 nm photolysis as well implying that a significant portion of the oxygen atoms produced in the photolysis process will correspond to NO(v=0). For NO(v=0), the corresponding O atoms have a kinetic energy of 1570 cm^{-1} in the O+OCS center-of-mass (c.m.) system. This amount is barely sufficient to overcome the activation energy to reaction. In the case of NO(v=1), oxygen will only have 600 cm^{-1} of kinetic energy in the O+OCS c.m. Since this insufficient to overcome the activation barrier, the only collisions that will lead to products are those in which the oxygen atom corresponds to NO(v=0). Thus, the reactive collisions will be essentially monoenergetic. The energy available for partitioning among product degrees of freedom from such reactive collisions is E_{avail} = 19,240 cm^{-1}.

In order to analyze the recorded CO transient signals, it is first necessary to devise a kinetic scheme that models the relevant formation and relaxation processes occurring within the reaction cell. A simplified model is given in the following list of elementary reactions.

$$O^* + OCS \rightarrow CO(v,J) + SO \qquad (1a)$$

$$O^* + OCS \rightarrow CO(v',J') + SO \qquad (1b)$$

$$O^* + M \rightarrow O + M \qquad (2)$$

$$CO(v,J) + M \rightarrow \sum_{v',J'} CO(v',J') + M \qquad (3a)$$

$$\sum_{v',J'} CO(v',J') + M \rightarrow CO(v,J) + M \qquad (3b)$$

Reaction 1a represents production of CO into the state being monitored with reaction 1b representing CO production into all other energetically accessible states. Reaction 2 represents deactivation or removal of translationally hot oxygen atoms from the probed volume without producing CO. This includes flight of oxygen out of the probed volume as well as the possible reaction with other species such as NO_2 or CO. Reactions 3a and 3b represent relaxation either out of or into the monitored CO state. Because of the

summations within reactions 3a and 3b, it is not possible to explicitly solve the set of differential equations resulting from this model, but if the relaxation processes are modelled by a two state system in which the monitored state interacts with a "bath" state consisting of all other possible CO states via k_{3a} and k_{3b}, then the following expression for the time-dependent concentration of CO(v,J) may be derived:

$$[CO(v,J,t)] = \frac{[O^*]_o [OCS] \left(C_r k_{1a} - (k_{1a}+k_{1b}) k_{3a} [M] \right)}{C_r \left(C_3 - C_r \right)} \left(\exp\{-C_r t\} - \exp\{-C_3 t\} \right)$$

$$+ \frac{[O^*]_o [OCS] \ (k_{1a}+k_{1b}) k_{3a} [M] \right)}{C_r C_3} \left(1 - \exp\{-C_3 t\} \right) \qquad (4)$$

where $C_r = (k_{1a}+k_{1b})[OCS] + k_2[M]$ and $C_3 = (k_{3a}+k_{3b})[M]$. In the limit as $t \rightarrow 0$, Equation 4 reduces to a simple expression linear in time:

$$[CO(v,J,t)] \approx k_{1a} [O^*]_o [OCS] \, t \qquad (5)$$

Equation 5 indicates that at times shorter than the relaxation rates, the nascent CO[v,J] population is linearly proportional to the initial slope of a plot of the CO absorption signal versus time.

CO product state distributions from the O + OCS → CO + SO reaction were determined by fitting the initial 500 μs of signal to line using a linear least-squares routine. The slope of the fitted line was recorded as the raw CO(v,J) population. However, since the technique employed absorption spectroscopy which measures the population difference between the two quantum states involved in the probed transition, it is also necessary to correct the raw data for the population in the upper state. The initial ~ 3 μs of signal for several transient absorption signals at three different CO(0,J) lines is shown in Figure 1. For CO(J<15), the initial rise of the absorption signal is delayed for some time following the photolysis pulse. The magnitude of the delay was dependent upon the rotational quantum number of the line being monitored with delays up to ~ 0.6 μs for J < 5. As the rotational quantum number of the state increased, the length of the delay decreased. For J ≥ 15, the rise of the absorption signal began promptly with the photolysis pulse.

A Boltzmann plot of the CO(v=0) rotational distribution as determined above is given in Figure 2. The plot exhibits a definite bimodal behavior. The high J distribution has a rotational temperature of $T_R = 4400 \pm 390$ K. The low J portion of the distribution is fit by $T_R = 350 \pm 20$ K. The CO lines that contribute to the low J distribution are those that show a delay in the initial rise of the absorption signal. The fact that the low J distribution has a rotational temperature close to room temperature, and the rise of the signals for these lines was delayed from the photolysis pulse suggest that the low J distribution is the result of rotational relaxation of the nascent CO distribution. However, the prompt rise of the absorption signals following photolysis at higher J's indicates that the above analysis is a

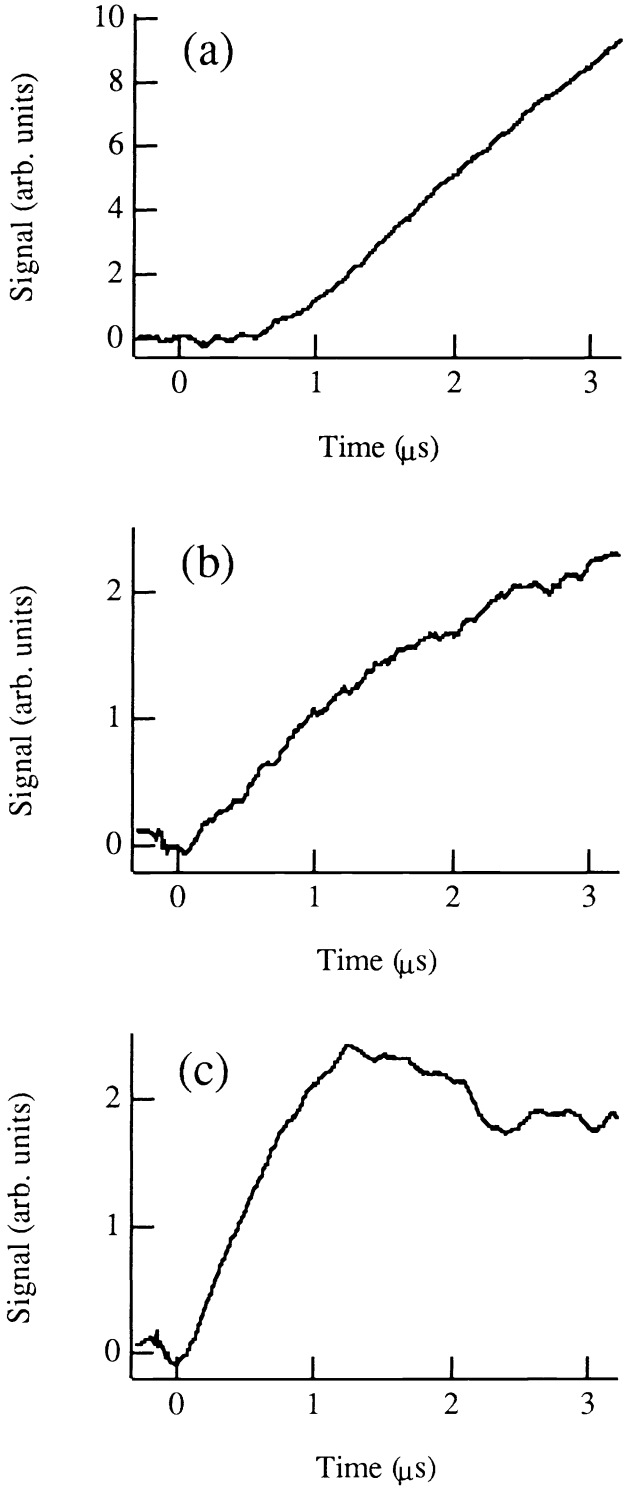

Figure 1. Transient absorption signals for (a) CO[v=0,R(5)], (b) CO[v=0,R(18)], and (c) CO[v=0,R(36)]. t = 0 indicates the photolysis pulse.

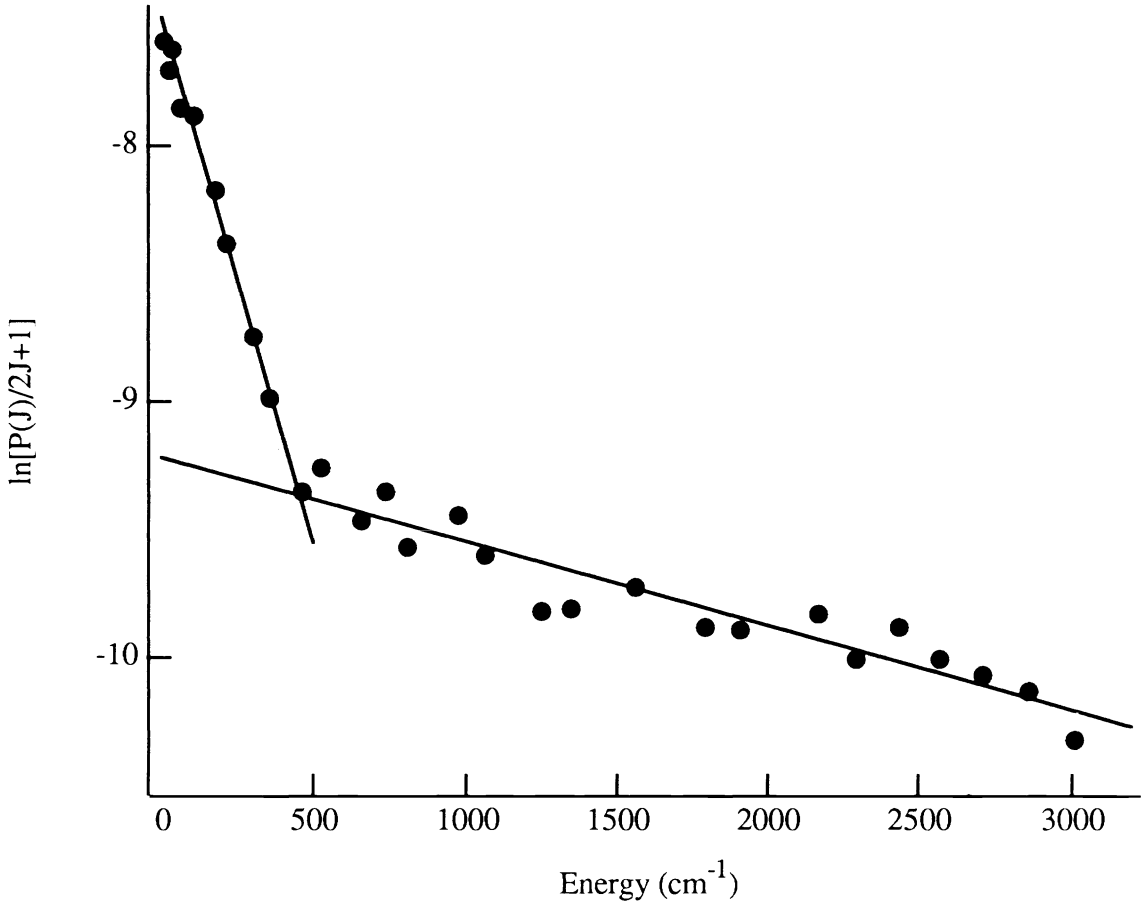

Figure 2. CO(v=0) Boltzmann plot. The low J portion of the plot is fit by a rotational temperature of $T_R = 350 \pm 20$ K, and the high J portion is fit by $T_R = 4400 \pm 390$ K. Error bounds in this and subsequent plots are expressed as $\pm \sigma$.

valid method for extracting the nascent populations from experimental data, *i.e.*, the data used to determine the nascent distributions is from the initial portion of the transient signals where relaxation processes have yet to significantly affect the populations.

The extent of statistical behavior of the CO(v=0) distribution was examined by comparing the measured distribution to a "prior" distribution in which the partitioning of energy among product degrees of freedom is constrained to maximize the entropy of the reaction. This was done using surprisal analysis in which $-\ln[P(J)/P^o(J)]$ is plotted versus a reduced energy variable, g_R, where P(J) is the experimentally measured distribution, $P^o(J)$ is the "prior" distribution, and g_R is given by $E_R(J)/(E_{avail}-E_v)$.[6] The slope of such a plot, given as Θ_R, is a measure of the statistical behavior of the distribution. If $\Theta_R < 0$, there is more energy partitioned into rotations than would be statistically expected; if $\Theta_R = 0$, the distribution behaves statistically; and if $\Theta_R > 0$, the distribution is colder than expected.

A surprisal plot of the CO(v=0) distribution is shown in Figure 3. The high J distribution has a surprisal parameter of $\Theta_R = 3.7 \pm 0.5$. Thus, the nascent CO(v=0) distribution is colder than statistically expected indicating that energy is being partitioned into other product degrees of freedom at the expense of CO rotations. The extremely large surprisal parameter of $\Theta_R = 76.1$ for the low J portion of the distribution is not surprising; once collisions significantly affect the product distribution, a comparison between the nascent CO distribution and a statistical distribution with $E_{avail} = 19{,}240$ cm^{-1} is no longer valid as the relaxation process reduces the total energy of the CO ensemble as CO comes into thermal equilibrium with the bath gases.

Very weak transient signals were observed in the CO(v=1) manifold for $J \leq 17$. A Boltzmann plot for CO(v=1) is given in Figure 4. The resulting distribution has a rotational temperature of $T_R = 340 \pm 55$ K. Because no signals were observed at higher J in the v = 1 manifold, it was not necessary to correct the CO(v=0) distribution for population in v = 1. Using the low J distributions of each level, a vibrational branching ratio was estimated to be $[v=1]/[v=0] \leq 0.05$. From these nascent CO(v,J) distributions an average energy content of the CO product was calculated to be $\langle E_{int}(CO) \rangle = 3150$ cm^{-1} which is 16% of the available energy.

The low relative energy content of CO indicates that the processes which determine energy partitioning within the reaction products are not statistical in nature. Additionally, the internal degrees of freedom of product CO are not in thermal equilibrium, *i.e.*, a temperature of 4400 K measured for the CO(v=0) rotational distribution would produce a vibrational branching ratio of $[v=1]/[v=0] = 0.5$. This is an order of magnitude greater than the vibrational branching ratio estimated above.

There are several possible hypotheses for the reaction dynamics which might explain the observed CO energy partitioning. The first is one in which the reactants form a long-lived $OCSO^{\dagger}$ complex as they traverse the PES. In the O + OCS reaction of the present study, the energy of collision is barely above the activation barrier so that a reactive

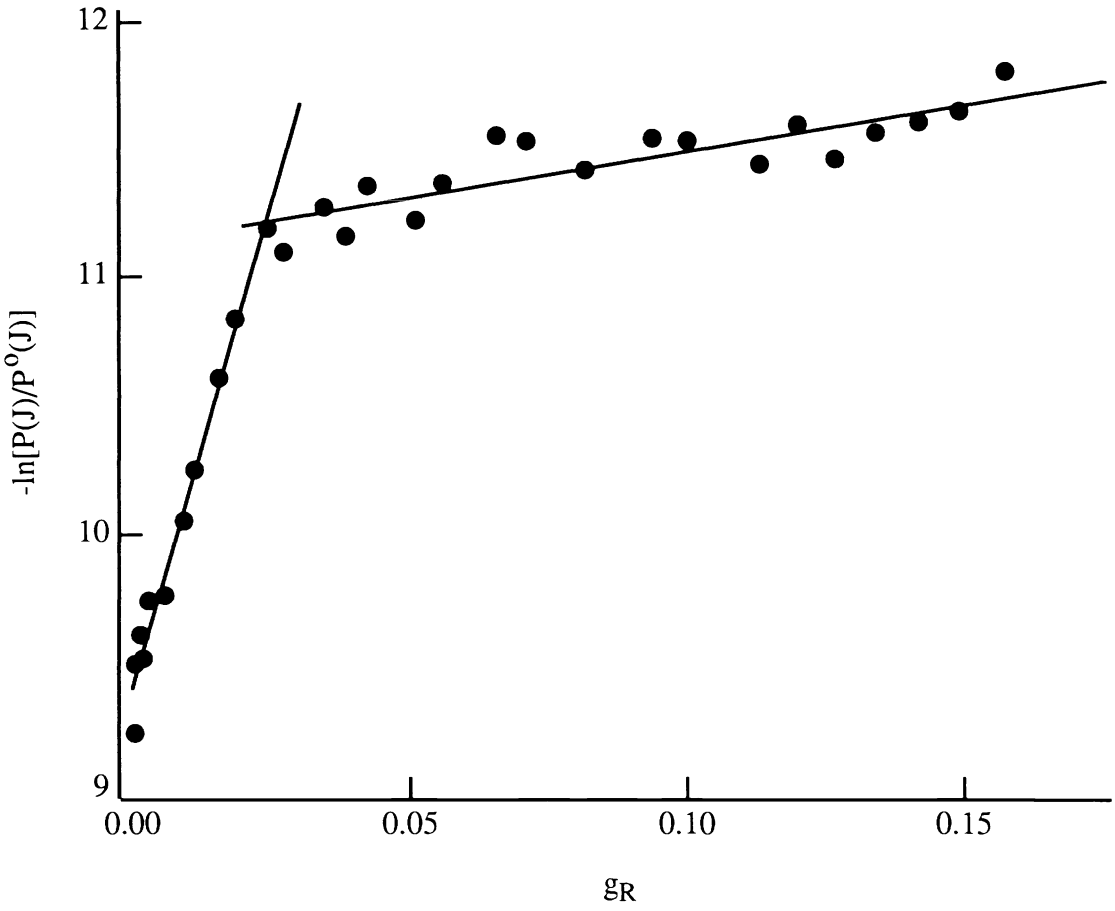

Figure 3. CO(v=0) surprisal plot. The low J portion is fit results in a surprisal parameter of $\Theta_R = 67.1$, and the high J portion is fit by $\Theta_R = 3.7 \pm 0.5$.

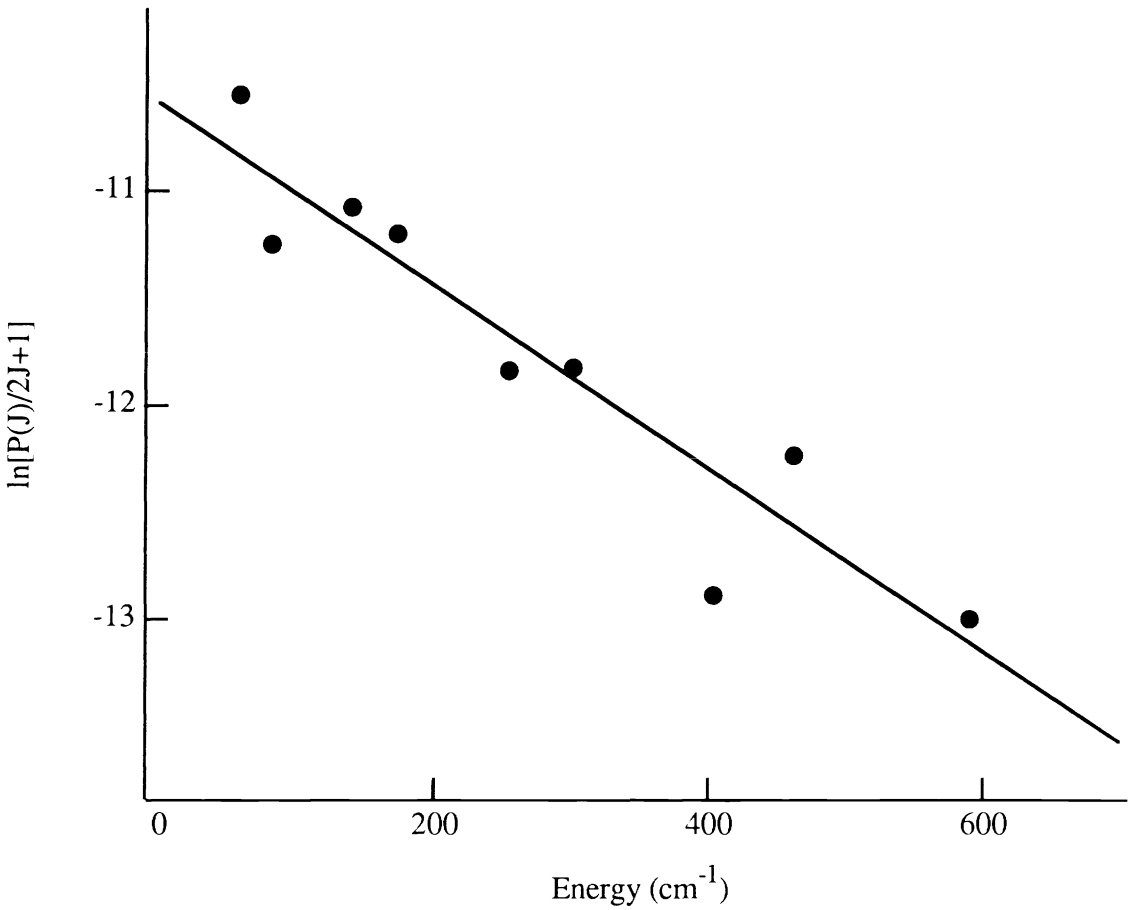

Figure 4. CO(v=0) Boltzmann plot. The plot has rotational temperature of T_R = 340 ± 55 K.

intermediate could form with little energy in its internal degrees of freedom, unlike previous studies in which the energy of the initial impact was well above the activation barrier of reaction making it unlikely that a local minimum along the reaction pathway of the PES was significantly affecting the final state distributions.[3,4] In such an intermediate, randomization of the energy available at the transition state would occur before the complex dissociates to products. In this scheme, excitation of the CO product is the result of a torque acting on CO in the exit channel as energy is released.

In the second hypothesis, the reactants traverse the transition state on a time scale short enough that complete energy randomization in the $OCSO^{\dagger}$ complex cannot occur, but rather energy is preferentially deposited into a degree of freedom that becomes the rotational motion of product CO. In this case, the $OCSO^{\dagger}$ complex dissociates before a significant amount of energy can flow into the CO vibrational mode. The release of energy in the exit channel is governed by the repulsive forces acting between the product c.m.'s and is directed primarily into the translational motion of the separating fragments.

Further experiments on this system are necessary in order to completely elucidate the dynamics of reaction. The energy content and product state distributions of the SO product must be determined. The amount of energy partitioned into product translations must be measured. It is also essential to calculate an accurate theoretical model of the O + OCS PES in order to determine whether a minimum exists along the reaction pathway corresponding to a stable intermediate $OCSO^{\dagger}$ complex as well as to examine the forces acting on the products within the exit channel. Additionally, trajectory calculations on such a model would establish the existence of a preferred collision geometry leading to reaction.

SUMMARY

1. The CO(v=0) rotational distribution was bimodal. The high J portion of the distribution had a rotational temperature of $T_R = 4400 \pm 390$ K and represent the nascent CO population. The low J distribution had a temperature of $T_R = 350 \pm 20$ K and was the result of rotational relaxation of the nascent distribution.

2. Surprisal analysis of the CO(v=0) distribution resulted in a surprisal parameter of $\Theta_R = 3.7 \pm 0.5$ indicating that the nascent CO(v=0) rotational distribution was colder than predicted by a statistical model in which the entropy in the products is maximized.

3. The CO(v=1) rotational distribution had a temperature of $T_R = 340 \pm 55$ K. Signals were not seen in this vibrational manifold for $J > 17$.

4. A vibrational branching ratio of $[v=1]/[v=0] \leq 0.05$ was determined using the low J distributions.

5. The average energy content of the CO product was $\langle E_{int}(CO) \rangle = 3150\ cm^{-1}$ which is only 16% of the available to product degrees of freedom.

REFERENCES

1. (a) I. Glassman, *Combustion*, Academic Press, New York, 1977. (b) P. Warneck, *Chemistry of the Natural Atmosphere*, Academic Press, San Diego, 1988.

2. (a) R. Atkinson, D.L. Baulch, R.A. Cox, R.F. Hampson Jr., J.A. Kerr,and J. Troe, *J. Phys. Chem. Ref. Data*, p. 881, Vol. 18, 1989. (b) W.B. DeMore, D.M. Golden, R.F. Hampson, C.J. Howard, M.J. Kurylo, M.J. Molina, A.R. Ravishankara, and S.P. Sander, *Chemical Kinetic and Photochemical Data for Use in Stratospheric Modeling, Evaluation Number 8*, JPL Publication 87-41, 1987.

3. S.L. Nickolaisen, H.E. Cartland, and C. Wittig, "CO Internal Excitation from the Reaction: $H + CO_2 \rightarrow CO + OH$," *J. Chem. Phys.*, submitted.

4. S.L. Nickolaisen, *State Resolved Product Dynamics in Atom-Molecule Interactions*, Doctoral dissertation, University of Southern California, 1991.

5. G.E. Busch and K.R. Wilson, "Triatomic Photofragment Spectra. I. Energy Partitioning in NO_2 Photodissociation," *J. Chem. Phys.*, pp. 3626-3638, Vol. 56(7), 1972.

6. R.D. Levine and R.B. Bernstein, *Molecular Reaction Dynamics and Chemical Reactivity*, Oxford University Press, New York, 1987.